



Design and synthesis of HIV-1 protease inhibitors for a long-acting injectable drug application

Bart Kesteleyn^{a,*}, Katie Amssoms^a, Wim Schepens^a, Geerwin Hache^a, Wim Verschueren^a, Wim Van De Vreken^a, Klara Rombauts^a, Greet Meurs^a, Patrick Sterkens^a, Bart Stoops^a, Lieven Baert^a, Nigel Austin^a, Jörg Wegner^a, Chantal Masungi^a, Inge Dierynck^a, Stina Lundgren^b, Daniel Jönsson^b, Kevin Parkes^b, Genadiy Kalayanov^b, Hans Wallberg^b, Åsa Rosenquist^b, Bertil Samuelsson^b, Kristof Van Emelen^a, Jan Willem Thuring^a

^aJanssen Infectious Diseases, A Division of Janssen Pharmaceutical Companies of Johnson & Johnson, Turnhoutseweg 30, 2340 Beerse, Belgium

^bMedivir AB, P.O. Box 1086, SE-141 22 Huddinge, Sweden

ARTICLE INFO

Article history:

Received 26 September 2012

Revised 18 October 2012

Accepted 22 October 2012

Available online 1 November 2012

Keywords:

HIV/AIDS

HIV Protease

Protease inhibitor

Long-acting formulation

Nanosuspension

ABSTRACT

The design and synthesis of novel HIV-1 protease inhibitors (PIs) (**1–22**), which display high potency against HIV-1 wild-type and multi-PI-resistant HIV-mutant clinical isolates, is described. Lead optimization was initiated from compound **1**, a Phe–Phe hydroxyethylene peptidomimetic PI, and was directed towards the discovery of new PIs suitable for a long-acting (LA) injectable drug application. Introducing a heterocyclic 6-methoxy-3-pyridinyl or a 6-(dimethylamino)-3-pyridinyl moiety (R^3) at the *para*-position of the P1' benzyl fragment generated compounds with antiviral potency in the low single digit nanomolar range. Halogenation or alkylation of the metabolic hot spots on the various aromatic rings resulted in PIs with high stability against degradation in human liver microsomes and low plasma clearance in rats. Replacing the chromanolamine moiety (R^1) in the P2 protease binding site by a cyclopentanolamine or a cyclohexanolamine derivative provided a series of high clearance PIs (**16–22**) with EC_{50} s on wild-type HIV-1 in the range of 0.8–1.8 nM. PIs **18** and **22**, formulated as nanosuspensions, showed gradual but sustained and complete release from the injection site over two months in rats, and were therefore identified as interesting candidates for a LA injectable drug application for treating HIV/AIDS.

© 2012 Elsevier Ltd. All rights reserved.

Since the introduction of antiretroviral (ARV) combination therapy, HIV/AIDS has become a manageable but chronic condition that requires lifelong treatment and compliance with the prescribed therapy.¹ Non-compliance may lead to drug plasma concentrations that are insufficient to suppress viral replication and the build-up of viral resistance, and this is one of the major factors contributing to treatment failure.^{2–4}

Long-acting (LA) formulations have recently been introduced as an alternative to the daily oral regimens in HIV treatment.⁵ LA intramuscular depot formulations generate sustained minimal but effective inhibitory concentrations of antiviral drug in the blood over a period of time, and offer the advantage of improved adherence to ARV therapy. Moreover, LA formulations have the potential to reduce adverse effects over time and may serve as a practical means of pre-exposure prophylaxis.

Typically, LA formulations consist of an active ingredient that is suspended in an oil-based solution or suspension (e.g., haloperidol depot), a microfine watery suspension (e.g., steroid depot), or a

suitable matrix from which the active ingredient is slowly released (e.g., Risperidal® Consta®). Nanosuspensions, (i.e., suspension formulations of drug particles in the nanosize range) allow the integration of poorly water- and oil-soluble drug substances in injectable LA formulations. Nanosizing may improve the dissolution rate of poorly soluble compounds and the release rate of the drug substance from the depot formulation.⁶

The HIV-1 protease enzyme is an attractive antiretroviral drug target for the treatment of HIV/AIDS, as it plays an essential role in the viral assembly and maturation process required for the production of infectious virus particles.⁷ With 10 protease inhibitors (PIs) approved for clinical use by the FDA since 1995, these compounds have an established role as a major component in ARV combination therapy.⁸ HIV-1 PIs typically occur as peptidomimetic competitive inhibitors of HIV-1 aspartic protease.⁹ Examples of marketed HIV-1 PIs include lopinavir, atazanavir and darunavir (Fig. 1).

The drug properties required for a new HIV-1 PI for a LA drug application differ substantially from those for an oral application. Slow release of the drug from the depot formulation is expected to provide sustained but low plasma concentrations. At these low

* Corresponding author. Tel.: +32 14641652; fax: +32 14605737.

E-mail address: bkestele@its.jnj.com (B. Kesteleyn).

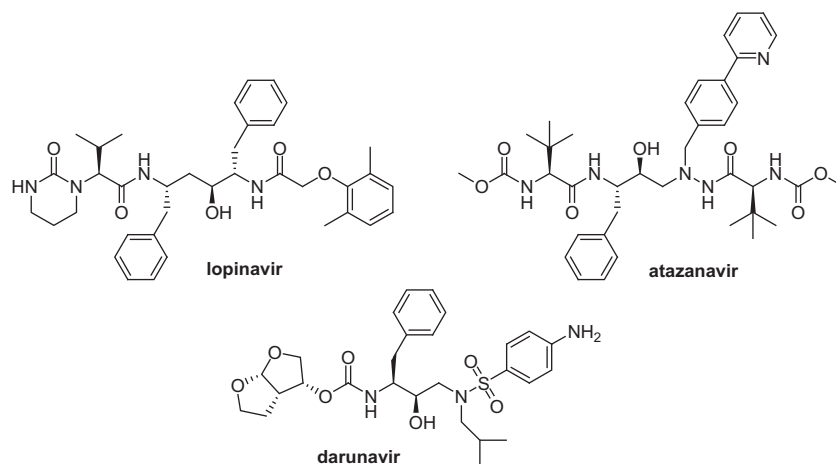


Figure 1. Structures of the marketed HIV-1 protease inhibitors lopinavir, atazanavir and darunavir.

concentrations, the drug must still suppress the viral replication of HIV-1 wild-type and mutant viruses. It is therefore believed that important requirements for a LA application include: (1) ultra-high potency against wild-type HIV, (2) high potency against multi-PI-resistant HIV-mutant clinical isolates, and (3) low functional plasma protein binding (PPB), as determined by the shift in EC_{50} value in the presence of 50% human serum in the antiviral assay. Also, with respect to the pharmacokinetic properties of the drug, (4) a high stability against microsomal degradation, resulting in low plasma clearance, might increase circulating drug levels in the plasma. Finally, (5) a low aqueous solubility of the drug is necessary, to limit the dissolution rate of the drug from the depot formulation.

In a lead-finding exercise, compound **1** was identified as an interesting PI scaffold to initiate a lead optimization program for a LA HIV-1 PI application (Fig. 2).

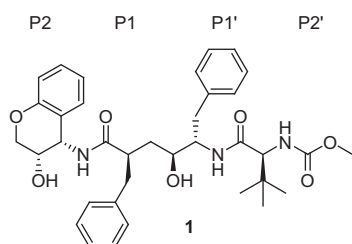


Figure 2. Structure of lead compound **1** with indication of the HIV-protease binding sites (P-sites).

Compound **1** is an example of the so-called Phe-Phe hydroxy-ethylene peptidomimetic scaffold for HIV-1 PIs, decorated with a chromanolamine moiety in the P2 position and a *t*-butylglycine fragment, similar to atazanavir, in P2'.^{10,11} The history of this scaffold goes back to the early days of HIV-1 PI research at Merck and the former Ciba-Geigy, which led to several preclinical and clinical candidates that have been evaluated up to Phase I clinical trials.^{12–16} Poor oral bioavailability seems to have hampered the development of this class of inhibitors.

As shown in Table 1, compound **1** was found to be a potent inhibitor of wild-type HIV-1, with an EC_{50} of 10 nM. Remarkably, it also displayed equal potency against a panel of mutant isolates (M_1 , M_2 and M_3) and in the presence of 50% human serum. The multi-PI-resistant mutants M_{1-3} contain combinations of known PI primary resistance-associated mutations (RAMs) reported by IAS,¹⁷ and each induces—to a certain extent—resistance against the marketed PIs lopinavir, atazanavir and darunavir, as shown in Table 1. Hence, these data indicate a low sensitivity of compound **1** to reported primary RAMs for PIs combined with low binding to plasma proteins; characteristics that match our postulated drug requirements (1), (2) and (3) for a LA PI drug application. The turnover of compound **1** by human liver microsomes (HLM) was fast (99% metabolized by HLM in 15 min, see Table 2). Also, *in vivo* in rats, compound **1** was rapidly cleared from the plasma following intravenous dosing ($Cl_{rat} = 4.0$ L/h/kg, see Table 2).

Detailed analysis of the metabolites generated by HLM degradation of compound **1** indicated that the aromatic moieties in positions P1 and P1', and the chromanolamine moiety in position P2,

Table 1
Antiviral activity against wild-type HIV-1_{IIIb} and HIV-mutant clinical isolates M_{1-3}

Compound	HIV-1 _{IIIb} ^a EC_{50} , nM	HIV-1 _{IIIb} ^b + 50%HS EC_{50} , nM	M_1 ^c EC_{50} , nM (FC)	M_2 ^c EC_{50} , nM (FC)	M_3 ^c EC_{50} , nM (FC)
Lopinavir	13	63	110 (9)	310 (23)	32 (3)
Atazanavir	6.8	13	57 (8)	3.2 (<1)	61 (9)
Darunavir	6.6	17	12 (2)	51 (8)	2.4 (<1)
1	10	19	19 (2)	6 (<1)	7 (<1)
11	1.7	6	1.3 (<1)	0.9 (<1)	0.8 (<1)
15	1.8	6.8	5.4 (3)	3.3 (2)	1.5 (<1)
18	0.8	2	0.8 (<1)	0.3 (<1)	0.5 (<1)
22	1.1	3.7	0.9 (<1)	0.6 (<1)	0.4 (<1)

^a The EC_{50} values were determined using MT4 cells. All EC_{50} values are reported as averages of at least two independent experiments (typically three to four) in which each assay was conducted in quadruplicate. Toxicity was measured in MT4 cells. CC_{50} values were >10 μ M for all compounds.

^b The antiviral EC_{50} value for HIV-1, measured in the presence of 50% human serum (50% HS) was used to determine functional plasma protein binding.

^c Mutant virus isolates M_1 , M_2 and M_3 contain the following PI resistance-associated mutations (bold figures represent primary resistance mutations, according to IAS¹⁷): M_1 : L10I, **M46I**, I64V, **I84V**, **L90M**, I93L; M_2 : L10I, I13V, **M46I**, **I50V**, L63P, **L76V**; M_3 : L10I, K20R, M36I, **G48V**, I62V, A71V, **V82A**, I93L. The numbers in parentheses represent the fold change (FC) in EC_{50} value for each mutant virus relative to wild-type HIV-1.

are metabolic hot spots (data not shown). Based on these observations, part of our lead optimization strategy was aimed at blocking all metabolic sites, mainly by halogenation at various positions on the aromatic moieties in the molecule. In addition, to improve the potency of the lead compound **1**, we envisioned introducing a heterocyclic aromatic moiety R^3 at the *para*-position of the P1' benzyl fragment, following the example of atazanavir.¹⁸

As outlined in Table 2, following the proposed lead optimization strategy to block metabolic hot spots, the benzyl moiety was decorated with an *ortho*-F, *ortho*-Cl or *meta*-OCF₃ substituent (R^2) in all new PIs. The introduction of a heterocyclic aromatic group (R^3) allowed for a substantial increase of antiviral potency, as exemplified by compounds **2** and **3**, which hold a methoxypyridine (MP) or dimethylaminopyridine (DMAP) moiety, respectively. These MP and DMAP fragments were selected from an extensive screen of alkyl-, alkoxy- and dialkylamino-substituted pyridines, pyrimidines, pyrazines and thiazoles as R^3 moieties. The MP and DMAP fragments provided the best overall compound profiles in terms of antiviral potency, effect on functional plasma protein binding, and microsomal stability. However, introducing a fluorine atom in P1 and a heterocyclic fragment R^3 induced only a minor reduction in metabolic turnover by HLM for compounds **2** and **3**. Blocking the remaining metabolic hot spot at the chromanolamine fragment, by introducing a *para*-chloro atom in compound **4**, was required to obtain a serious reduction of microsomal turnover and a reduction of plasma clearance in rats. The microsomal turnover by HLM could be reduced to virtually zero by replacing the *ortho*-F atom in P1 by an *ortho*-Cl (compound **5**) or *meta*-OCF₃ (compound **6**) substituent, but no further reduction in plasma clearance in rats was observed for these compounds. Also, these P1 modifications did not benefit the antiviral potency of compounds **5** and **6**, particularly when measured in the presence of 50%HS.

In a further effort to fine-tune the compound properties, a series of chromanolamine derivatives with fluoro-, chloro- and methyl-substituents at positions 6 and 8 (R'' and R' respectively, in compounds **7–15**) were synthesized. As an overall trend, blocking the R'' -position with a halogen was found to be beneficial for metabolic stability and to provide lower plasma clearance in rats. The combination of a fluorine atom at R'' and a chloro- or methyl-substituent at R' (compounds **11** and **15**, respectively), provided the best overall profile; this included potent antiviral activity (also in the presence of 50%HS) and low functional plasma clearance in rats. In the case of compound **11**, the presence of a DMAP substituent (R^3) was found to be more favorable than MP (compound **10**), in terms of antiviral potency and plasma clearance in rats.

As mentioned above, for a LA drug application, the plasma concentrations that can be obtained by slow sustained release from a nanosuspension depot formulation are expected to be very low in practice. It is crucially important that the drug is able to suppress the virus (wild-type HIV-1, as well as the mutant clinical isolates) at these concentrations. Ultra-potent (preferably sub-nanomolar) inhibitors of wild-type HIV-1, with good coverage of resistant mutants, are therefore required.

To this end, we noticed that replacing the chromanolamine moiety in P2 by small lipophilic cyclopentanolamines or cyclohexanolamines provided a series of compounds (**16–22**) with potent antiviral activity against wild-type HIV-1 (EC₅₀ range of 0.8 – 1.1 nM). The effect was most pronounced for compounds **18** and **22**, which have a (*R*)-3-methyl-cyclohexanolamine and a thiophene-cyclohexanolamine moiety, respectively, in the P2 position. However, all compounds in this series had high microsomal turnover and were rapidly cleared from the plasma in rats. Replacing the *ortho*-F R^2 -substituent by *ortho*-Cl (compound **20**), or *meta*-OCF₃ (compound **21**), did not reduce the microsomal turnover, as was the case for compounds **5** and **6** with the 6-chloro-chromanolamine

moiety in P2. Also, replacing the R^3 -fragment MP by a DMAP group (compound **19**) did not improve any drug properties with respect to those of compound **18**.

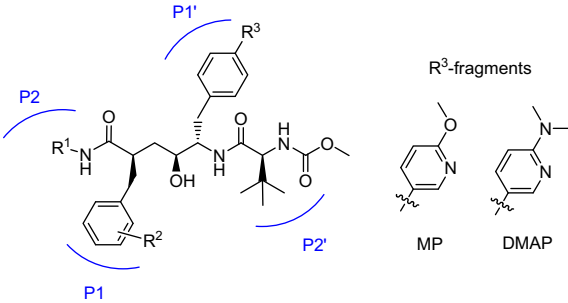
In conclusion, our SAR exploration of the Phe–Phe hydroxyethylene peptidomimetic PI scaffold afforded two compound series with distinct compound properties. Compounds **11** and **15** are the most potent (antiviral activity on HIV-1_{IIIB} in the presence of 50%HS) 'low clearance' PIs. Compounds **18** and **22**, on the other hand, represent the most potent 'high clearance' PIs. These four compounds, with the R^1 -substituent as the major structural differentiator, were taken forward in a comparison of their resistance profiles and LA pharmacokinetic properties.

All new HIV-1 PIs (**1–22**) were synthesized according to the reaction sequence outlined in Scheme 1. The synthesis of compound **1** was started from lactone **28a** ($R = H$). For compounds **2–22**, the introduction of an aromatic moiety (R^3), typically via a Suzuki coupling reaction, required the presence of a bromo-substituent at the *para*-position of the P1 benzyl group of the lactone, and thus required the synthesis of the halogenated lactone **28b** ($R = Br$). The synthesis of lactone **28a** ($R = H$) has previously been described elsewhere.^{19,20} For the synthesis of the bromo-lactone **28b** ($R = Br$), a new enantioselective methodology was developed. As shown in Scheme 2, the synthesis started from commercially available *N*-Boc-protected (*S*)-4-bromophenylalanine **23**. After conversion of the carboxylic acid group to the Weinreb amide **24**, substitution with the Grignard reagent 3-butenylmagnesium bromide provided ketone **25**. Oxidation of the terminal double bond with catalytic RuCl₃·3H₂O and excess NaIO₄ afforded the γ -keto-carboxylic acid **26**. After conversion of compound **26** to the corresponding methyl ester **27** with methyl iodide, and using potassium bicarbonate as a mild base, reductive cyclization with *N*-selectride in THF at low temperature afforded the desired bromo-lactone **28b** in high enantiomeric excess (ee >95%).

Alkylation of lactones **28a** or **28b** with substituted benzyl bromides (**29**), using lithium hexamethyldisilazane as a base at low temperature, afforded *trans*-alkylation products **30**.²¹ Hydrolysis of compound **30** with NaOH or LiOH in methanol-water, and subsequent quenching by acidification to pH = 3 with citric acid, provided the carboxylic acid derivative **31**. Spontaneous re-lactonization of compound **31** was prevented by silylation of the alcohol group with TBDMSCl to intermediate **32**. In order to create a diversity of examples of PIs **1–22**, the introduction of the P2 amine and the R^3 substituents was accomplished by the HATU-mediated coupling of amines **33** and subsequent palladium-assisted Suzuki coupling of boronic acids **35** (except for compound **1**). Finally, *N*-Boc deprotection under acid conditions, or using a combination of TMSCl and NaI in acetonitrile, was followed by HATU-mediated coupling of *N*-(methoxycarbonyl)-*L*-tert-leucine (**38**), to provide the desired HIV-1 PIs **1–22** in high overall yields and enantioselective purity (ee >95%). In some cases it proved advantageous to postpone deprotection of the silyl-protecting group until after the Suzuki-coupling reaction, to avoid degradation by the elimination of water. This degradation reaction was observed particularly in the case of Suzuki-coupling reactions that required longer reaction times. Also, the introduction of the R^3 aromatic moiety can be performed as early as the first step in the reaction scheme—at the stage of compound **28b**—or be postponed until the final step in the reaction scheme, using virtually the same Suzuki-coupling reaction conditions as described in the general scheme.

All halogenated and alkylated chromanolamine P2 derivatives **45b–j** were prepared by adaptation of a procedure formerly reported for the synthesis of chromanolamine **45a**.²² As shown in Scheme 3, *ortho*- and/or *para*-substituted phenols **39** were converted to the corresponding chromanon derivatives **41** by *O*-alkylation with 3-bromopropionic acid and subsequent Friedel–Crafts cyclization of intermediates **40**. In several cases, a

Table 2
SAR overview for HIV-1 protease inhibitors **1–22**



Compound	R ¹ -amine	R'	R''	R ²	R ³	HIV-1 _{IIIIB} ^a EC ₅₀ , nM	HIV-1 _{IIIIB} ^b + 50%HS EC ₅₀ , nM	HLM ^c %Metab.	Cl _{rat} ^d L/h/Kg
1				H	H	10	19	99	4.0
2				o-F	MP	2.5	6.6	72	5.8
3				o-F	DMAP	1.5	10	90	9.1
4				o-F	MP	2.7	14	23	0.47
5				o-Cl	MP	3.9	13	5	1.4
6				m-OCF ₃	MP	4.2	24	0	-
7		R'	R''	o-F	MP	2.4	5.3	47	3.9
8		Cl	H	o-F	MP	1.2	5.8	48	2.1
9		F	H	o-F	MP	2.8	6.9	98	5.3
10		Cl	F	o-F	MP	2.6	8.4	8	1.9
11		Cl	F	o-F	DMAP	1.7	6	22	0.8
12		F	Cl	o-F	MP	4.1	16	23	-
13		H	Me	o-F	MP	0.9	7.7	63	2.8
14		F	Me	o-F	MP	2.8	9.8	48	5
15		Me	F	o-F	MP	1.8	6.8	17	1.6
16				o-F	MP	1.1	3.3	99	4.7
17				o-F	MP	1.8	5.9	99	5.2
18				o-F	MP	0.8	2.0	99	5.4
19				o-F	DMAP	1.1	4.9	99	5.6
20				o-Cl	MP	1.1	7.1	99	4.2
21				m-OCF ₃	MP	0.9	3.2	94	5.4
22				o-F	MP	1.1	3.7	91	4.8

^a The EC₅₀ values were determined using MT4 cells. All EC₅₀ values are reported as averages of at least two independent experiments (typically three to four), in which each assay was conducted in quadruplicate. Toxicity was measured in MT4 cells. CC₅₀ values were >10 μM for all compounds.

^b The antiviral EC₅₀ value for HIV-1, measured in the presence of 50% human serum (50% HS), was used to determine functional plasma protein binding.

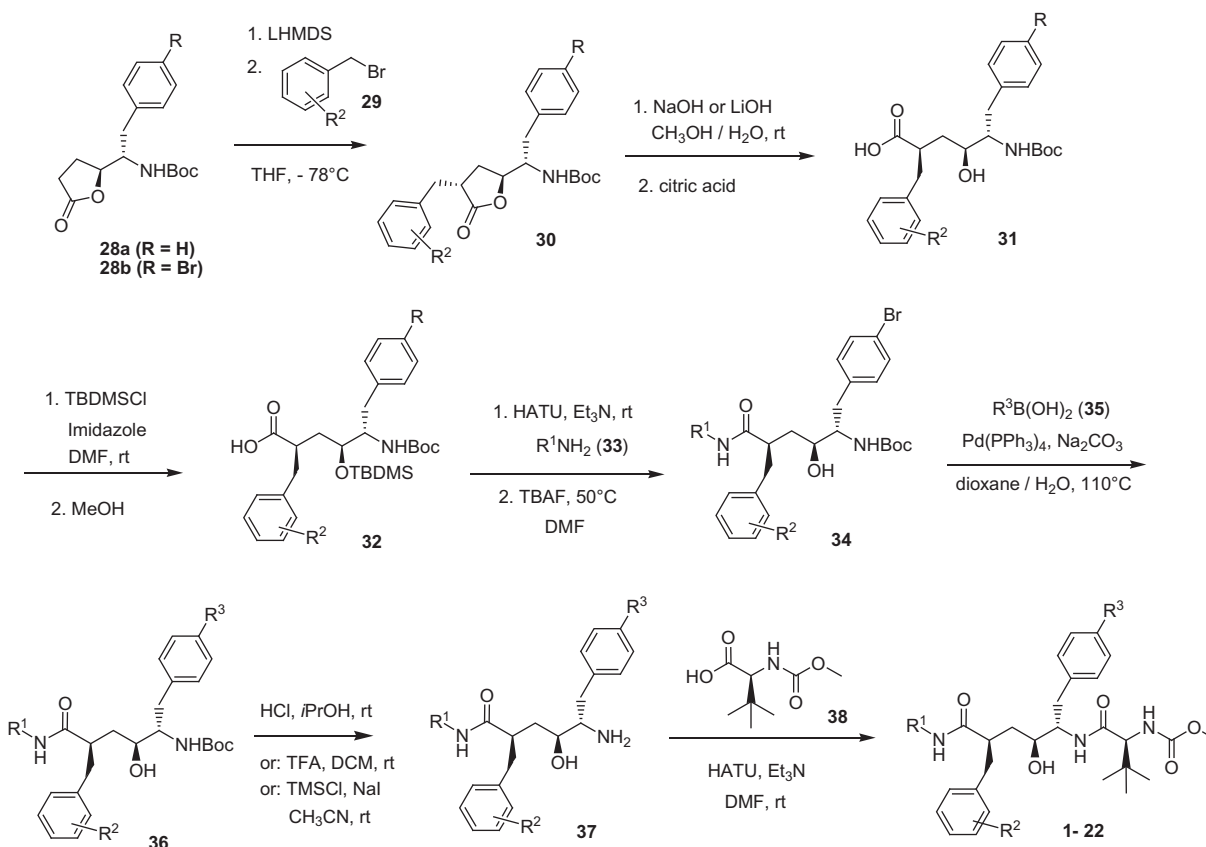
^c Metabolic turnover by HLM (human liver microsomes) is represented as the %compound metabolized at a concentration of 1 μM after 15 min, incubated at 37 °C.

^d Plasma clearance in rats (Cl_{rat}) was determined after intravenous dosing of 2 mg/kg compound in a suitable formulation, typically 1 mg/mL in a mixture of PEG400/ethanol/saline at a ratio of 70/20/10. Reported clearance figures are averages taken from two or three animals. Clearance from plasma in rats higher than 70% of the liver blood flow (Cl_{rat} > 3 L/h/kg) is ranked as 'high'. Compound extraction from plasma in rats below 30% of the liver blood flow (Cl_{rat} < 1.3 L/h/kg) is ranked as 'low'.

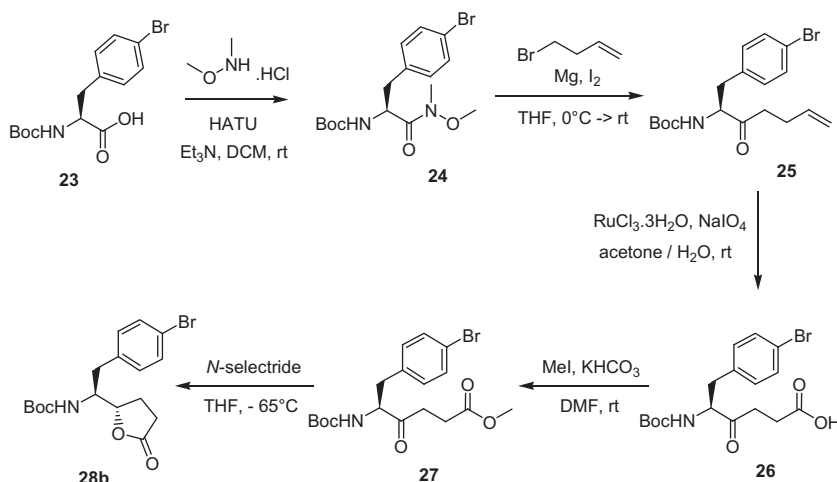
two-step alternative procedure was used to prepare intermediates **40**: NaH-mediated alkylation with 3-chloropropanol, followed by oxidation of the primary alcohol with TEMPO and bis(acetoxy)iodobenzene (BAIB), providing higher overall yields of intermediates **40**. Reaction of chromanones **41** with bromine in dichloromethane afforded a mixture of the mono- and di-brominated reaction products **42** and **43**. Upon treatment of this mixture with sodium sulfite in acetic acid at 70 °C, the di-brominated intermediates **42** were selectively reduced to the mono-brominated intermediates **43**. After reduction with sodium borohydride, bro-

mohydrines **44** were submitted to a Ritter reaction using sulfuric acid in acetonitrile to provide, after hydrolysis of the cyclic intermediate oxazolidines, the *cis*-substituted chromanolamines **45** as racemic mixtures. The enantiomers **45** were separated via chiral SFC. The absolute stereochemistry was assigned by vibrational circular dichroism (VCD), by comparing the recorded VCD spectra of both enantiomers with those obtained by computational *ab initio* calculation.²³

(1*R*,2*S*,3*R*)-2-amino-3-methylcyclopentanol, the R¹-fragment of compound **16**, was prepared as previously described elsewhere.²⁴

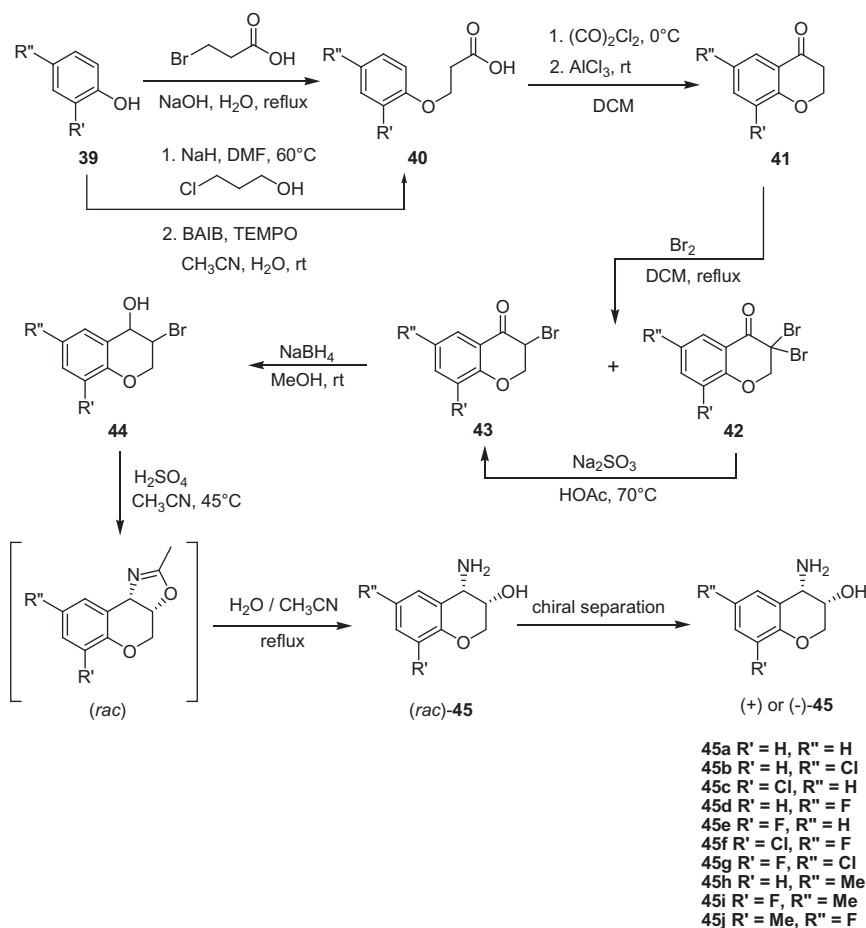


Scheme 1. Synthesis of protease inhibitors 1–22.

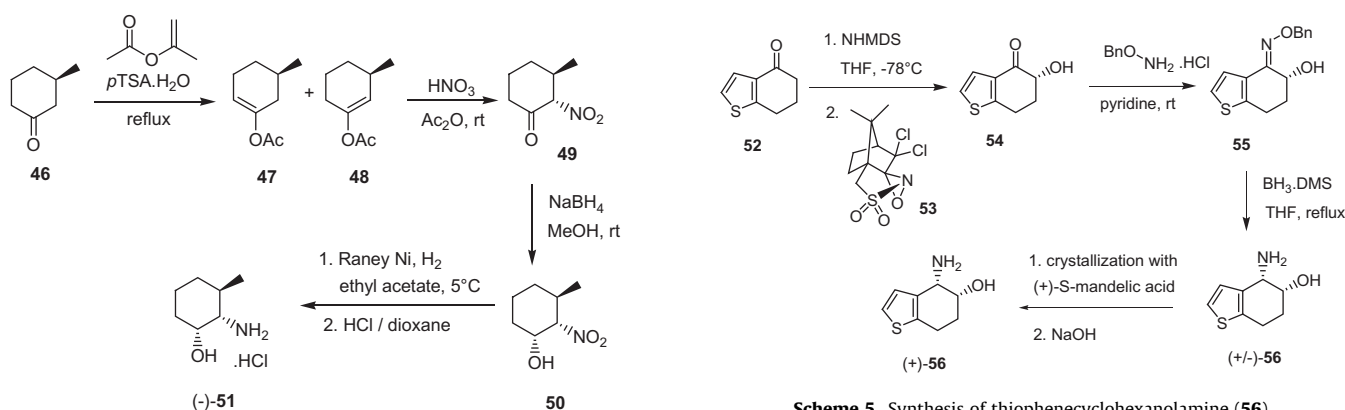
Scheme 2. Synthesis of bromo-lactone (**28b**).

Enantioselective synthesis of the chiral P2 methylcyclohexanolamine fragment **51** was found to be rather challenging, especially with regard to stereo control of the amino and alcohol substituents on the cyclohexane ring. Several reaction steps in the sequence provided mixtures that required tedious chromatographic separation. As shown in Scheme 4, the synthesis of compound **51** was started from commercially available 3*R*-methylcyclohexanone (**46**). Acid-catalyzed *O*-acetylation of compound **46** with isopropenyl acetate afforded a non-separable mixture of compounds **47** and **48** in a ratio

of 10:7. Treatment of the mixture with concentrated nitric acid in acetic anhydride afforded a mixture of all four possible nitrated reaction products. The desired 2*S*-nitro-3*R*-methylcyclohexanone (**49**), the major component in the mixture, was separated by chromatography over silica gel, and isolated in an overall yield of 11% from compound **46**. Reduction of the carbonyl group of compound **49** with sodium borohydride afforded a 1:1 epimeric mixture of alcohols, and required chromatographic separation to provide the desired *cis*-nitro-alcohol intermediate **50** in a yield of 22%. Finally, after reductive



Scheme 3. Synthesis of chromanolamine derivatives (45a–j).



Scheme 5. Synthesis of thiophenecyclohexanolamine (56).

Scheme 4. Synthesis of methylcyclohexanolamine (51).

hydrogenation of the nitro group, methylcyclohexanolamine **51** was isolated as the hydrochloric acid salt with an ee >95% (as determined by SFC analysis after conversion to the corresponding Mosher amide).

For the synthesis of the thiophenecyclohexanolamine P2 fragment **56**, an enantioselective route was developed as depicted in Scheme 5. The procedure uses the chiral oxidation reagent camporsulfonyloxaziridine (**53**) for the asymmetric alpha-oxidation of commercially available 6,7-dihydro-5H-benzo[b]thiophen-4-one (**52**), as reported earlier for the alpha-hydroxylation of chromanone enolates.²⁵ Condensation of compound **54** with *O*-benzyl-hydroxyamine and subsequent diastereoselective reduction

with borane afforded an enantiomerically enriched mixture (ee = 60%) of thiophenecyclohexanolamines **56**. The pure enantiomer (+)-**56** (ee >95%) was obtained by recrystallization of its *S*-mandelic acid salt from methanol. The absolute stereochemistry was confirmed by VCD.

Pls **11**, **15**, **18** and **22** were tested against a panel of HIV-mutant clinical isolates (M₁, M₂ and M₃) (Table 1). Compared to the marketed drugs lopinavir, atazanavir and darunavir, compounds **11**, **15**, **18** and **22** performed better overall against wild-type HIV-1 and the resistant mutants, in terms of both absolute potency and fold changes (FC) of the EC₅₀ value relative to the activity on wild-type HIV-1. Virtually no resistance to any of the mutant

Table 3
Nanosuspension composition, particle size, dose and bioavailability in rats of compounds **11**, **18** and **22**

Compound	Nanosuspension composition	d ₁₀ ^a (nm)	d ₅₀ ^a (nm)	d ₉₀ ^a (nm)	Dose (mg/kg)	F _{IM} ^b (%)
18	100 mg/mL of Compound 18 and 25 mg/mL polysorbate 20 (tween20) and 9 mg/mL NaCl in water	75	128	211	37.5	>100
22	50 mg/mL of Compound 22 and 12.5 mg/mL poloxamer 338 (Pluronic F108) and 50 mg/mL sucrose in water	78	125	219	41	>100
	50 mg/mL of Compound 22 and 15 mg/mL Vit-E TPGS in water	72	123	213	40	100
11	100 mg/mL of Compound 11 and 25 mg/mL polysorbate 20 (tween20) and 15 mg/mL NaCl in water	67	123	219	50	3
	50 mg/mL of Compound 11 and 25 mg/mL poloxamer 338 (Pluronic F108) and 50 mg/mL sucrose in water	64	120	213	30	5
	50 mg/mL of Compound 11 and 25 mg/mL Vit-E TPGS and 1 mg/mL DSPG and 50 mg/mL sucrose (in 0.15 M NaCl) in water	72	122	207	30	12

^a d_{10–50–90}: the size of particle for which 10%, 50% and 90% of the sample is below this size. Particle sizes of the nanosuspensions were measured by laser diffraction with a Beckman Coulter LS230 diffractometer (Beckman Coulter, Inc., Fullerton, CA, USA).

^b F_{IM}: absolute bioavailability of the intramuscular (IM) route. Bioavailability was assessed after 1 month of sampling, and was determined as ((AUC_{IM} × dose_{IV})/(AUC_{IV} × dose_{IM})) × 100.

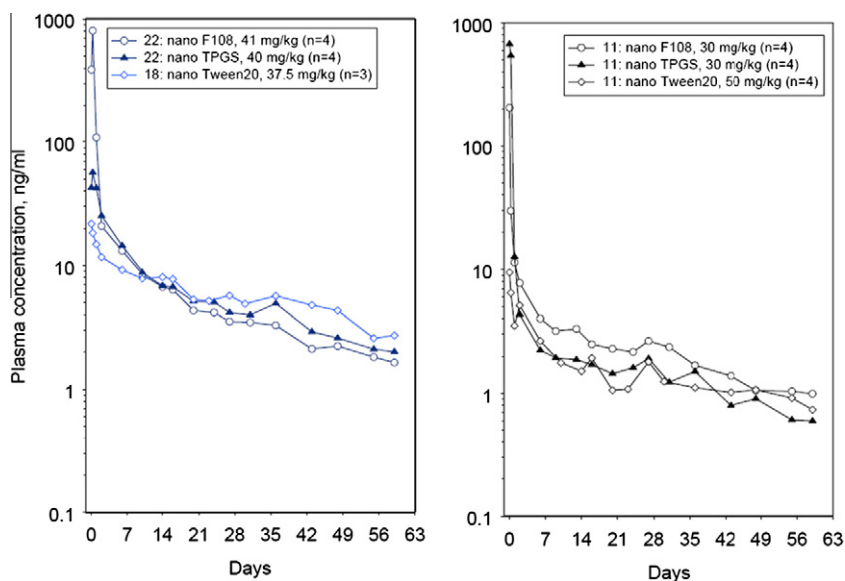


Figure 3. Mean plasma concentration profiles (ng/mL) of compound **11**, **18** and **22** long-acting nanosuspensions in rats after IM dosing.

isolates was observed for compounds **11**, **18** and **22**, and LA pharmacokinetic profiles were generated for these three most interesting PIs.

For an injectable nanosuspension depot formulation, the pharmacokinetic compound release profiles typically depend partly upon the nanocrystal particle size distribution and the surfactant used to stabilize the formulation, but mainly upon the intrinsic physico-chemical properties of the compound, such as the aqueous solubility of the crystal form (polymorph). Therefore, the low clearance (**11**) and the two high clearance (**18**, **22**) PIs were recrystallized and isolated as stable crystalline polymorphic forms. The aqueous solubility of all polymorphs was found to be less than 100 µg/mL. Using Elan's NanoCrystal technology,²⁶ sterile nanosuspensions were prepared by continuous wet milling of the crystals in an aqueous carrier containing a hydrophilic surfactant, resulting in nanocrystals with a particle size of less than 200 nm. As shown in Table 3, several non-ionic surfactants were evaluated as additives for the LA nanosuspension formulations: (1) poloxamer 338 (Pluronic F108), (2) D- α -tocopheryl polyethylene glycol 1000 succinate (Vit-E TPGS), and (3) polysorbate 20 (tween20). The nanosuspension LA depot formulations were injected intramuscularly (IM) in rats. Blood samples were taken at regular intervals over a period of two months after dosing, and the compound release profiles in plasma and absolute bioavailability (F_{IM}) were determined.

Figure 3 shows the LA pharmacokinetic profiles for the low clearance (**11**) and two high clearance (**18** and **22**) PIs. Overall, the plasma concentration profiles for the three compounds were found to be quite similar, providing low but sustained drug concentration in the plasma over a period of two months. As an overall observation regarding the effect of the surfactant on compound release profiles, the nanosuspension formulations stabilized with surfactants Tween20 (for compounds **11** and **18**) and Vit-E TPGS (for compound **22**) provided a more gradual compound release profile than the formulations based on Pluronic F108. Such LA PK profiles, characterized by a lower initial burst and low peak (C_{max}) to trough (C_{min}) ratio, may offer the advantage of higher efficacious compound concentrations in the plasma, less frequent dosing, and reduced safety issues.

With regard to bioavailability (F_{IM}), compounds **18** and **22** both reached a bioavailability of 100% as indicated in Table 3, suggesting complete dissolution of the nanosuspensions from the injection site. The bioavailability of the low clearance compound **11**, however, remained low (F_{IM} < 12%) after applying several different types of additive to the nanosuspension formulation. As a result of the limited bioavailability of compound **11**, the postulated hypotheses of the potential beneficial effect of reduced clearance on the concentrations of circulating drug could not be evaluated. As a possible explanation, limited solubility and/or permeability may have hampered the release of compound **11** from the injection

site. Despite the high plasma clearance properties of compounds **18** and **20**, sustained plasma concentrations well above EC₅₀ values were obtained for both compounds following single dosing.

With respect to synthetic efficiency, the synthesis of PI **22** (outlined in Schemes 1, 2 and 5) requires a total of 15 reaction steps but can nevertheless be accomplished with an overall yield of 9%. On the contrary, the current low-yielding procedure for the synthesis of the methylcyclopentanolamine building block **51** (Scheme 4), leads to a poor overall yield for the synthesis of PI **18**. Nevertheless, taking into account the high intrinsic antiviral potency against HIV wild-type, the high activity against a panel of multi-PI-resistant HIV-mutant clinical isolates and the favorable long-acting pharmacokinetic properties, PIs **18** and **22**, formulated as nanosuspensions, are interesting candidates for a LA injectable drug application for the treatment of HIV/AIDS.

References and notes

- Bartlett, J. A.; DeMasi, R.; Quinn, J.; Moxham, C.; Rousseau, F. *AIDS* **2001**, *15*, 1369.
- Fogarty, L.; Roter, D.; Larson, S.; Burke, J.; Gillespie, J.; Levy, R. *Patient Educ. Couns.* **2002**, *2*, 93.
- Rathbun, C.; Farmer, K.; Stephens, J. R.; Lackhart, S. M. *Clin. Ther.* **2005**, *27*, 199.
- Sethi, A. K.; Celentano, D. D.; Gange, S. J.; Moore, R. D.; Gallant, J. E. *Clin. Infect. Dis.* **2003**, *37*, 1112.
- Baert, L.; Van't Klooster, G.; Dries, W.; François, M.; Wouters, A.; Basstanie, E.; Iterbeke, K.; Stappers, F.; Stevens, P.; Schueller, L.; Van Remoortere, P.; Kraus, G.; Wigerinck, P.; Rosier, J. *Eur. J. Pharm. Biopharm.* **2009**, *72*, 502.
- Rabinow, B. E. *Nat. Rev. Drug Disc.* **2004**, *3*, 785.
- Kohl, N. E.; Emini, E. A.; Schleif, W. A.; Davis, L. J.; Heimbach, J. C.; Dixon, R. A. F.; Scolnick, E. M.; Sigal, I. S. *PNAS* **1988**, *85*, 4686.
- Martinez-Cajas, J. L.; Wainberg, M. A. *Antiviral Res.* **2007**, *76*, 203.
- Tsantrizos, Y. S. *Acc. Chem. Res.* **2008**, *41*, 1252.
- Vacca, J. P.; Guare, J. P.; deSolms, S. J.; Sanders, W. M.; Giuliani, E. A.; Young, S. D.; Darke, P. L.; Zugay, J.; Sigal, I. S.; Schleif, W. A.; Quintero, J. C.; Emini, E. A.; Anderson, P. S.; Huff, J. R. *J. Med. Chem.* **1991**, *34*, 1225.
- Lyle, T. A.; Wiscourt, C. M.; Guare, J. P.; Thompson, W. J.; Anderson, P. S.; Darke, P. L.; Zugay, J. A.; Emini, E. A.; Schleif, W. A.; Quintero, J. C.; Dixon, R. A. F.; Sigal, I. S.; Huff, J. R. *J. Med. Chem.* **1991**, *34*, 1228.
- Thompson, W. J.; Fitzgerald, P. M. D.; Holloway, M. K.; Emini, E. A.; Darke, P. L.; McKeever, B. M.; Schleif, W. A.; Quintero, J. C.; Zugay, J. A.; Tucker, T. J.; Schwering, J. E.; Homnick, C. F.; Nunberg, J.; Springer, J. P.; Huff, J. R. *J. Med. Chem.* **1992**, *35*, 1685.
- Lin, J. H.; Chen, I. W.; King, J. J. *Pharmacol. Exp. Ther.* **1992**, *263*, 105.
- Alteri, E.; Bold, G.; Cozens, R.; Faessler, A.; Klimkait, T.; Lang, M.; Lazdins, J.; Poncioni, B.; Rösel, J. L.; Schneider, P.; Walker, M.; Woods-Cook, K. *Antimicrob. Agents Chemother.* **1993**, *37*, 2087.
- Capraro, H.-G.; Bold, G.; Frässler, A.; Cozens, R.; Klimkait, T.; Lazdins, J.; Mestan, J.; Poncioni, B.; Rösel, J. L.; Stover, D.; Lang, M. *Arch. Pharm. Pharm. Med. Chem.* **1996**, *329*, 273.
- Cozens, R. M.; Bold, G.; Capraro, H.-G.; Fässler, A.; Mestan, J.; Lang, M.; Poncioni, B.; Stover, D.; Rösel, J. L. *Antiviral Chem. Chemother.* **1996**, *7*, 294.
- Johnson, V. A.; Calvez, V.; Günthard, H. F.; Paredes, R.; Pillay, D.; Shafer, R.; Wensing, A. M.; Richman, D. D. *Top Antiviral Med.* **2011**, *19*, 156.
- Bold, G.; Faessler, A.; Capraro, H.-G.; Cozens, R.; Klimkait, T.; Lazdins, J.; Mestan, J.; Poncioni, B.; Rösel, J.; Stover, D.; Tintelnot-Blomley, M.; Acemoglu, F.; Beck, W.; Boss, E.; Eschbach, M.; Huerlimann, T.; Masso, E.; Roussel, S.; Ucci-Stoll, K.; Wyss, D.; Lang, M. *J. Med. Chem.* **1998**, *41*, 3387.
- Evans, B. E.; Rittle, K. E.; Homnick, C. F.; Springer, J. P.; Hirshfield, J.; Veber, D. F. *J. Org. Chem.* **1985**, *50*, 4615.
- Degeoey, D. A.; Flentge, C. A.; Flosi, W. J.; Grampovnik, D. J.; Kempf, D. J.; Klein, L. L.; Yeung, M. C.; Randolph, J. T.; Wang, X. C.; Yu, S. U.S. Patent Appl. Publ. 2005, U.S. 20,050,148,623.
- Ghosh, A. K.; McKee, S. P.; Thompson, W. J. *J. Org. Chem.* **1991**, *56*, 6500.
- Cheng, Y.; Zhang, F.; Rano, T. A.; Lu, Z.; Schleif, W. A.; Gabryelski, L.; Olsen, D. B.; Stahlhut, M.; Rutkowski, C. A.; Lin, J. H.; Jin, L.; Emini, E. A.; Chapman, K. T.; Tata, J. R. *Bioorg. Med. Chem. Lett.* **2002**, *12*, 2419.
- Kuppens, T.; Bultinck, P.; Langenaeker, W. *Drug Discovery Today Technol.* **2004**, *1*, 269.
- Hungate, R. W.; Chen, J. L.; Starbuck, K. E. *Tetrahedron Lett.* **1991**, *32*, 6851.
- Davis, F. A.; Weismuller, M. C. *J. Org. Chem.* **1990**, *55*, 3715.
- Elan Drug Technologies, Nanocrystal Technology, Technology Focus Brochure, **2008**. Available from: <http://www.elan.com/EDT/nanocrystal_technology/> [Last accessed on 9 October, 2011].